J Mater Sci: Mater Electron (2016) 27:7540–7547
DOI 10.1007/s10854-016-4734-8

Low-temperature sintering of metallacyclic stabilized copper nanoparticles and adhesion enhancement of conductive copper film to a polyimide substrate

Tomonori Sugiyama[1] · Mai Kanzaki[1] · Ryuichi Arakawa[1] · Hideya Kawasaki[1]

Received: 29 February 2016 / Accepted: 22 March 2016 / Published online: 26 March 2016

Abstract We report that both low electric resistivity and strong adhesion to polyimide film were attained for a conductive Cu film prepared by low-temperature sintering of 2-amino-1-butanol-protected Cu nanoparticles (AB-Cu NPs) with an average size of 4.4 nm. The sintering temperature of 60 °C for the AB-Cu NPs is the lowest ever reported for Cu NPs. A nanoink comprising these AB-Cu NPs (~35 wt% Cu) produced a conductive Cu film with resistivity of 52 μΩ cm after heating at 150 °C under a nitrogen flow. The adhesion to a polyimide film was compared for films prepared from nanoinks consisting of three different types of alkanol-amine-based Cu NPs: AB-Cu NPs, 1-amino-2-propanol-Cu NPs, and 3-amino-1-propanol-Cu NPs. Only the Cu film prepared from the AB-Cu nanoink established strong adhesion to the substrate without decreasing the electrical conductivity. The adhesiveness is attributed to residual oxidation products after thermal sintering of the Cu nanoinks.

1 Introduction

Copper nanoparticles (Cu NPs) have been drawing research interest because of their potential application as the active material in conductive nanoinks [1], optical devices [2], catalysts [3], and antibacterial agents [4]. In particular, Cu-NP-based nanoinks have attracted much attention for their application in printed electronics on paper or flexible plastic substrates [5], whose latest advances have enabled fast, easy, and cost-effective creation of functional electronic devices. Silver nanoparticles are one of the promising materials for conductive nanoinks because of their high conductivity and oxidation resistance [6, 7]. However, silver is too expensive to be used in large quantities; moreover, silver electrical circuits are often hampered by electro-migration [8]. Cu NPs are regarded as a suitable alternative for conductive nanoinks because of their high conductivity, low cost, and reduced effect of electro-migration [9–22]. The major problem associated with Cu NPs is their low oxidation resistance in ambient air; the presence of copper oxide not only raises the sintering temperature, but also dramatically reduces the electrical conductivity of Cu NPs [5]. One of the critical technical challenges in realizing the manufacture of printed electronics is using a low-temperature (<150 °C) sintering process under to fabricate highly conductive Cu patterns ($<10^{-5}$ Ω cm) without reductive gas flow (e.g. hydrogen gas and formic acid) [17, 19], while also promoting the adhesion of the conductive film on a given substrate. However, these two requirements have incompatible characteristics: the addition of polymer binders (e.g. epoxy resin and ethyl cellulose) increases the adhesive force, but the electrical resistance of the Cu film is increased by the insulation properties of the binder [23].

In the present study, we developed a process for high-concentration (0.3 M Cu salt) synthesis of 2-amino-1-butanol (AB)-protected copper nanoparticles (AB-Cu NPs) in ethylene glycol at room temperature (~20 °C) under ambient air conditions. To ensure low-temperature sintering of Cu NPs on a flexible (polymeric) substrate, we

Electronic supplementary material The online version of this article (doi:10.1007/s10854-016-4734-8) contains supplementary material, which is available to authorized users.

✉ Hideya Kawasaki
hkawa@kansai-u.ac.jp

[1] Faculty of Chemistry, Materials and Bioengineering, Kansai University, 3-3-35 Yamate-cho, Suita 564-8680, Japan

fabricated sub-10-nm AB-Cu NPs with an average size of 4.4 ± 1.0 nm using a metallacyclic coordination stability [22, 24], since the melting or sintering temperature of Cu NPs significantly decreases with decreasing size in the sub-10-nm region [25]. Several approaches have been developed for the fabrication of sub-10-nm Cu NPs, using solution synthesis via chemical reduction of copper(II) salts in the presence of strongly-bounded organic ligands such as polymers and surfactants [26–29]. The sub-10-nm AB-Cu NPs developed in this study had more advanced characteristics required for conductive nanoinks: (1) very low sintering temperature of 60 °C; (2) low electrical resistivity of the order of 10^{-5} Ω cm was obtained after the low-temperature (<150 °C) sintering process under a nitrogen flow; (3) strong adhesion to a polyimide film without the addition of polymer binders. The adhesion enhancement of the AB-based Cu nanoink was investigated on the basis of the residual organic products after thermal sintering of the Cu nanoink and the effect of the primary and secondary types of alcohol used as alkanol-amine stabilizers of the Cu NPs.

2 Experimental section

2.1 Materials

All the chemicals were used as received without further purification. 2-amino-1-butanol (AB, 98 %), 1-amino-2-propanol (AmIP, 98 %), 3-amino-1-propanol (NPA, 98 %), copper(II) acetate anhydrate (97.0 %), propylene glycol (99.0 %), ethylene glycol (99.5 %), glycerol (99.0 %), ethanol (99.5 %), hydrazine monohydrate (98.0 %), *N*,*N*-dimethylacetamide (98.0 %), toluene (98.0 %), and hexane (96.0 %) were purchased from Wako Chemicals, Japan.

2.2 Synthesis of AB-Cu NPs and preparation of AB-Cu-NP-based nanoink

2.2.1 Synthesis

The AB-Cu NPs were synthesized in ethylene glycol with a high concentration of copper(II) acetate under ambient air conditions at room temperature (~20 °C), using AB as the stabilizer and hydrazine monohydrate as the reducing agent (molar ratio of Cu salt/AB/hydrazine = 1:10:10). In a typical process, 14.1 mL of AB was added to 28.6 mL of ethylene glycol. Next, 2.73 g of solid copper(II) acetate was added to the AB solution at the room temperature, producing a blue solution due to the formation of an AB-Cu complex. This solution had a high concentration (300 mM) of Cu salt. Then, 7.3 mL of hydrazine monohydrate was added to the blue solution in a single step, under stirring at 1100 rpm and at the room temperature. The colour of the resulting solution rapidly changed from blue to a blackish deep red. Stirring continued for about 24 h at 1100 rpm and the room temperature under an air atmosphere. After 24 h, the AB-Cu NPs were precipitated by adding *N*,*N*-dimethylacetamide to the colloidal dispersion of the Cu NPs, and the precipitates were washed with toluene and then hexane. The solution synthesis of AmIP-Cu NPs with an average size of 3.5 ± 1.0 nm and NPA-Cu NPs with an average size of 5.8 ± 1.0 nm was carried out according to the method described in our previous report [24].

2.2.2 Cu nanoink

The purified powder of the synthesized AB-Cu NPs was re-dispersed uniformly in a solvent mixture of propylene glycol and glycerol (1:1 v/v) to produce the Cu nanoink (~35 wt% Cu). The resulting Cu nanoink was kept in a freezer before use, and it remained stable for at least 2 months; no change was observed in the resistivity of the Cu conductive film prepared from the Cu nanoink 2 months after it was produced. The Cu nanoink was applied onto various polyimide films with a bar coater. The resulting Cu films were then sintered at various temperatures (50–200 °C) for 30 min in an electric furnace (FT-6000, FuLL-TECH, Osaka, Japan) under a N_2 gas flow of 1.1 L/min. The thickness of each Cu film after heating was determined by a surface roughness measuring tool (SJ 310, Mitutoyo, Japan), and the average thickness was calculated (~4 μm). The electrical resistivity of the Cu conductive films was analysed using a four-point probe (Loresta AX MCP-T370, Mitsubishi Chemical Analytech Co., Japan).

2.3 Characterization

Fourier-transform infrared (FT-IR) spectroscopy was performed using a spectrometer (FT-IR 4200, JASCO, Japan) coupled with units for attenuated total reflection. Transmission electron microscope (TEM; JEM-1210, JEOL, Japan) images were recorded at an acceleration voltage of 100 kV. Field-emission scanning electron microscope (FE-SEM; JSM-6700, JEOL, Japan) images were collected at an acceleration voltage of 5.0 kV. The surface morphology of the Cu film was determined by scanning it with an atomic force microscope (AFM; SPM-9700, Shimadzu, Japan) operated in the dynamic force microscopy mode. X-ray diffraction (XRD) patterns were obtained by a diffractometer (D2 Phaser, Bruker, Germany) with a Cu K_α radiation source ($\lambda = 1.5406$ Å). Thermo-gravimetric analysis (TGA) was performed using a TG analyser (Thermo plus EVO, Rigaku, Japan) at a heating rate of 10 °C/min under a nitrogen flow. The heat flow during

heating of the Cu nanoink was measured by a differential scanning calorimeter (DSC; Thermo plus DSC 8240, Rigaku, Japan) at a heating rate of 5 °C/min under a nitrogen flow.

3 Results and discussion

3.1 Characterization of AB-Cu NPs

Figure 1a shows a TEM image of the AB-Cu NPs, which were obtained by re-dispersion of the purified AB-Cu NP powder in ethanol. The AB-Cu NPs had a narrow size distribution and average size of 4.4 ± 1.0 nm, as shown in ESI Fig. S1. Figure 1b shows the XRD pattern of the AB-Cu NPs. A main diffraction peak emerges at $2\theta = 40°$–50°, which can be assigned to copper metal, Cu(0). The quite broad peaks at 2θ of 37° and 63° can be attributed to Cu(I) oxide (Cu_2O) produced by Cu surface oxidation. Thus, AB-Cu NPs comprise a main component of Cu(0) in the metallic core with the surface oxidation. The extremely broad peak indicates that the as-prepared AB-Cu NPs had a small size, which is consistent with the estimation of ~4 nm from the corresponding TEM image.

The IR spectra of the free AB ligands and AB-Cu NPs were acquired to clarify the presence of AB protective layers on the surface of the Cu NPs. Figure 2a shows the IR spectra in the range 800–4000 cm^{-1}. Similar to the IR spectrum of the free AB ligands, the IR spectrum of the AB-Cu NPs also exhibits characteristic absorption bands in the range of 2800–3000 cm^{-1} corresponding to the C–H stretching vibration of $–CH_3$ and $–CH_2$, while those in the range of 3100–3400 cm^{-1} correspond to the stretching vibration of O–H and N–H. This indicates that the Cu NPs were protected by the AB ligands. The difference between the N–H stretching vibration (3100–3400 cm^{-1}) and N–H bending (1550–1650 cm^{-1}) bands of the AB-Cu NPs and free AB ligands suggests the coordination of the amino and hydroxyl groups of the AB ligand with the surface of the Cu NPs.

The TGA analysis of the purified AB-Cu NPs demonstrated that most of the AB protecting layers decomposed at temperatures below 150 °C, as shown in Fig. 2b. The total mass loss was <42 %, which is assigned to loss of the AB ligands in Cu NPs. The gradual minor weight loss (2.8 wt%) that occurred between 150 and 320 °C reveals the presence of organic residual products inside the sintering Cu film obtained at heating temperatures below 300 °C.

3.2 DSC and XRD analysis: sintering behaviour of AB-Cu NPs

It has been reported that the sintering of Cu NPs with a size of 20 nm resulted in an exothermic process [30], which arose from minimization of the surface area during sintering. In the present study, thermal analysis of the sintering behaviour of sub-10-nm AB-Cu NPs was conducted by the DSC under a nitrogen flow (Fig. 3a). An exothermic peak appears between 60 and 150 °C in the thermogram of the AB-Cu NPs, and the area of this exothermic peak yields an enthalpy of 310 ± 35 J/g.

XRD spectra of the AB-Cu NPs were acquired after different heating temperatures (50, 90, 120, 150, 180, and 200 °C; Fig. 3b), and they confirm that low-temperature sintering of Cu NPs successfully occurred at 60 °C. The full width at half maximum (FWHM) of the major peak assigned to Cu (111) dramatically decreases between 50 and 90 °C, indicating that sintering of the AB-Cu NPs occurred in this temperature range. By applying Scherrer's equation to the FWHM of the diffraction peaks, we estimated the average crystallite size of copper at various

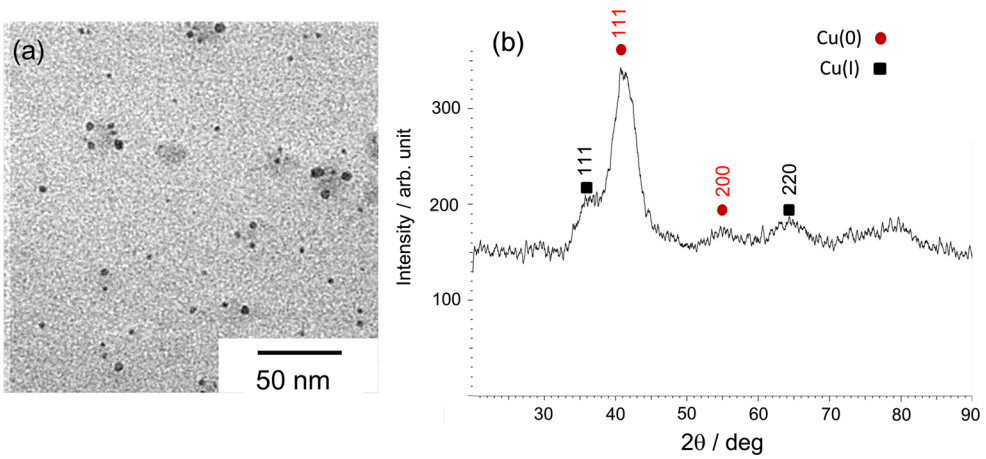

Fig. 1 **a** TEM image and **b** XRD pattern of AB-Cu NPs

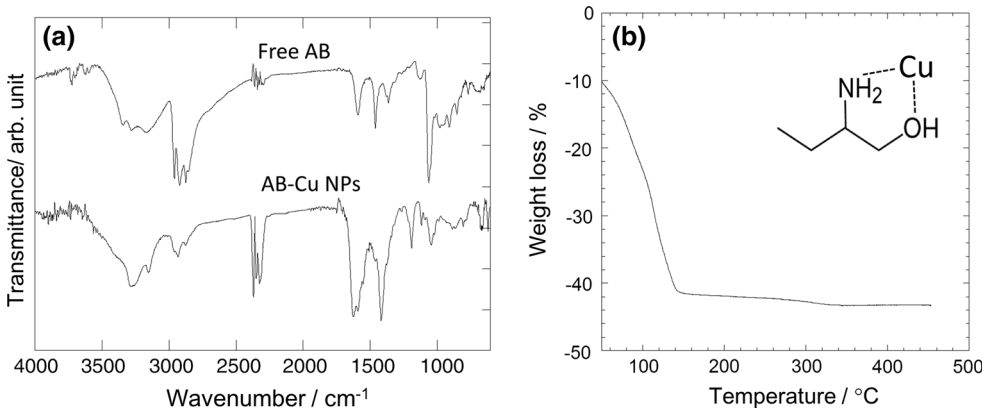

Fig. 2 **a** IR spectra of AB-Cu NPs and free AB. **b** TGA curve of AB-Cu NPs obtained at a heating rate of 10 °C/min under a N_2 flow. A schematic of the metallacyclic coordination stability of a five-membered ring type between Cu and AB is shown in the *inset*

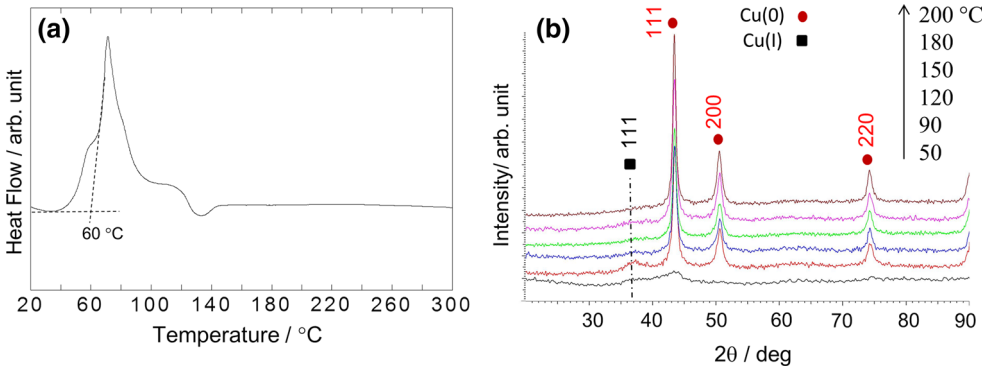

Fig. 3 **a** DSC curve of AB-Cu NPs at a heating rate of 5 °C/min under a N_2 flow. **b** XRD patterns of Cu films after thermal sintering of Cu nanoink (~35 wt% Cu, propylene glycol/glycerol solvent = 1:1 v/v) on polyimide film for 30 min at different temperatures: 50, 90, 120, 150, 180, and 200 °C

temperatures above 90 °C. Our results indicate that the crystallite size of AB-Cu NPs gradually increased at higher temperatures (ESI Fig. S2). The combined results of XRD and DSC analysis make it clear that sintering of the sub-10-nm AB-Cu NPs started at about 60 °C, which is much lower than the sintering temperature (~170 °C) of 20-nm Cu NPs [30]. The surface melting effect of metallic nanoparticles may be responsible for the low temperature-sintering of nanoparticles [31].

3.3 Electrical resistivity of the conductive copper film

We measured the electrical resistivity of the Cu films prepared from nanoinks based on AB-CuNPs (~35 wt% Cu) sintered at different temperatures between 90 and 200 °C for 30 min under a N_2 gas flow (1.1 L/min). The electrical resistivity of the Cu films dramatically decreased at 120 °C (Fig. 4), which is consistent with the initiation of the sintering (~60 °C) of AB-Cu NPs. It should be noted that the high electrical resistivity of the Cu film prepared at a heating temperature of 90 °C is attributed to the residual high-boiling-temperature solvents, propylene glycol and glycerol, in the Cu nanoink. The electrical resistivity further decreased as the heating temperature increased from

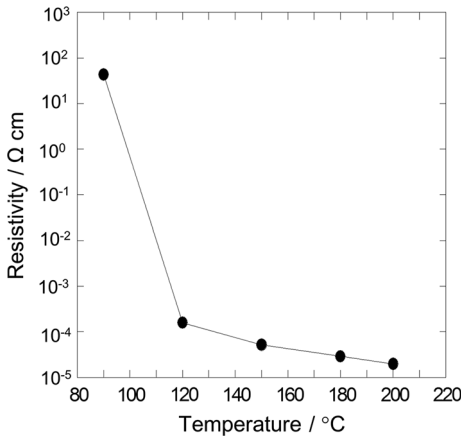

Fig. 4 Electrical resistivity of Cu films after the thermal sintering of Cu nanoink (~35 wt% Cu, propylene glycol/glycerol solvent = 1:1 v/v) on polyimide film for 30 min at 90, 120, 150, 180, and 200 °C

90 to 200 °C (43 ± 20 Ω cm at 90 °C; 158 ± 7.9 μΩ cm at 120 °C; 52 ± 3.1 μΩ cm at 150 °C; 29 ± 0.2 μΩ cm at 180 °C; 20 ± 1.7 μΩ cm at 200 °C) because the sintering and size growth of the Cu NPs continued to progress at higher heating temperatures.

The sintering and size growth of Cu NPs were confirmed by the corresponding FE-SEM images. Figure 5a–f show FE-SEM images of the Cu films obtained at different

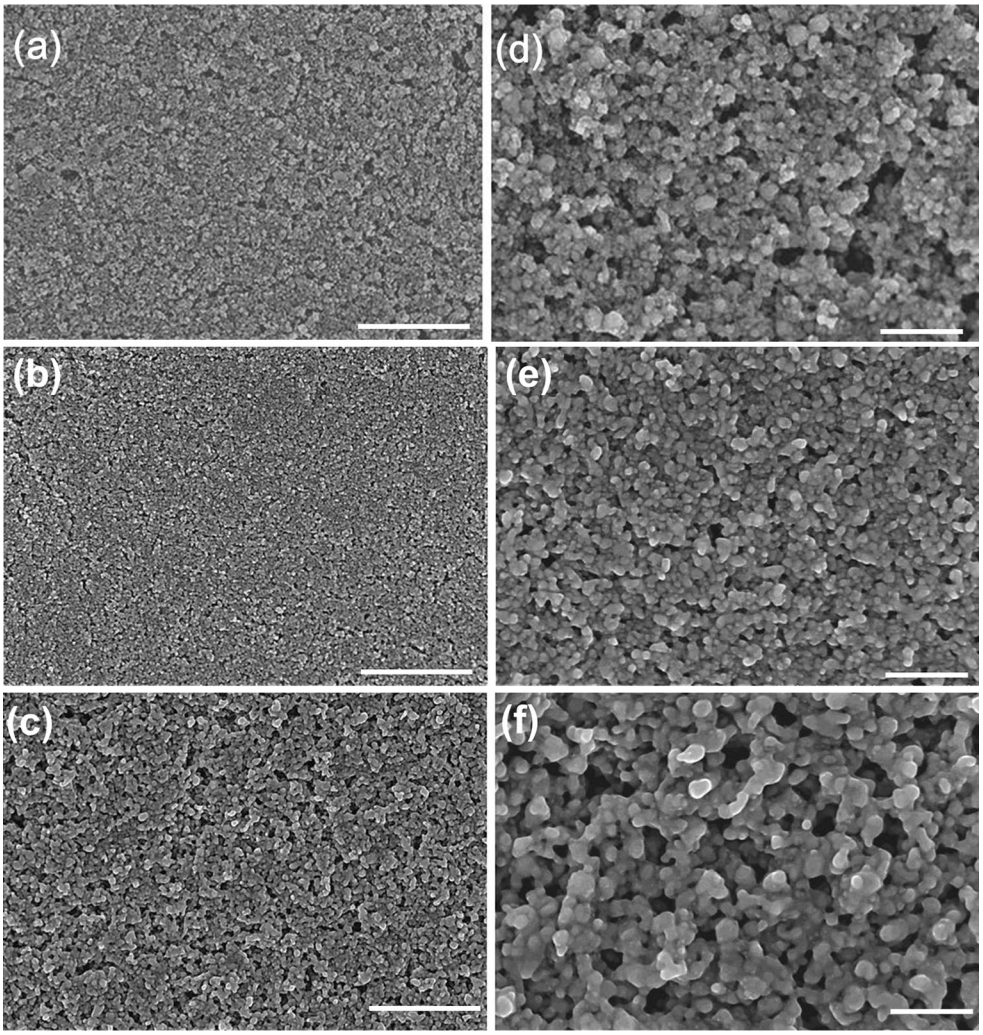

Fig. 5 FE-SEM images of Cu films after thermal sintering of Cu nanoink (~35 wt% Cu, propylene glycol/glycerol solvent = 1:1 v/v) on polyimide film for 30 min at **a**, **d** 120 °C, **b**, **e** 150 °C, and **c**, **f** 200 °C. The magnification of the images is ×30,000 in (**a**, **b**, **c**) and ×100,000 in (**d**, **e**, **f**). The *scale bar* of (**a**, **b**, **c**) is 1 μm; that of (**d**, **e**, **f**) is 100 nm

heating temperatures. At a heating temperature of 120 °C, the size of particles in the Cu film grew from 3–6 to 50–100 nm, while the electrical resistivity of the Cu film dramatically decreased, as shown in Fig. 4. Further progress in the size growth and the interconnection among particles was observed at 150 and 200 °C, accompanied by further decreases in the electrical resistivity. The AFM images of the conductive Cu films sintered at 150 and 200 °C also confirm that the sintering and particle-size growth proceeded at higher heating temperatures (ESI Fig. S3). The three-dimensional structures in the AFM images show that the arithmetic average roughness, R_a of the sintering Cu film increased from 9.1 nm at 150 °C to 20.7 nm at 200 °C.

It is worth mentioning that the low electrical resistivity of $\sim 5 \times 10^{-5}$ Ω cm at 150 °C can be obtained with the Cu NPs with surface oxidation, although the surface oxidation inhibits the necking of Cu NPs. We speculate that these oxides decomposed at higher temperatures of more than 120 °C, so that the necking can be formed among Cu NPs. Actually, the XRD patterns show a clear peak of copper oxide after sintering at 90 °C, but the oxide peak is obscure at higher temperatures of more than 120 °C. This is contrast to the general tendency on the enhanced surface oxidation of copper at higher temperatures [32]. The reason for this reduction of Cu(I) to Cu(0) may be the intrinsic reducing capacity of AB ligands.

3.4 Adhesion enhancement of Cu films on polyimide films through the use of AB-Cu-NP-based nanoink

A concern in the manufacture of printed circuitry is ensuring adhesion of the Cu film to a chosen substrate.

Copper films on polyimide (PI), Cu/Pi, has been widely used in the manufacture of flexible circuits. However, a critical issue for the Cu/PI system lies in the poor adhesion of Cu to PI films [33]. In order to strengthen the adhesion of the Cu film on different polymer substrates, the nanoinks generally contain polymeric binders such as epoxy-resin and ethyl-cellulose. However, the polymeric binders can affect the electrical conductivity of nanoinks after low-temperature sintering when its decomposition temperature is higher than the sintering temperature [34–37]. Therefore, we did not employ polymeric binders in our Cu-NP-based nanoink. Instead, we focused on the possibility of utilizing residual organic products as an adhesive agent inside the Cu film after thermal sintering of the Cu nanoink [38]. A cross-cut test (i.e. a measure of adhesion strength) was used to compare the adhesion of sintering Cu films prepared from different Cu-NP-based nanoinks to a PI film. Nanoinks were produced from three different types of alkanolamine-protected Cu NPs: AB-Cu NPs, AmIP-Cu NPs, and NPA-Cu NPs. The chemical structures of these alkanolamines are shown in Fig. 6a. The cross-cut test is one of the methods for determining the resistance of a coating as a function of its separation from the substrate; the test uses a tool to cut a right-angled lattice pattern in the coating [39]. Three Cu/PI films were prepared by thermal sintering of the Cu-NP based-nanoinks (~35 wt% Cu, propylene glycol/glycerol solvent = 1:1 v/v) at 150 °C for 30 min.

As shown in Fig. 6b, the Cu film prepared from the nanoink consisting of AmIP-Cu NPs displayed very poor adhesion to the substrate in the cross-cut test. Most of the Cu film flaked off in the first cross-cut test because most of the AmIP ligands were removed after thermal sintering. In contrast, the adhesion strength dramatically improved for the Cu film prepared from the nanoink consisting of AB-Cu NPs, as shown in Fig. 6c. Even after the third cross-cut test, the Cu film flaked only along the edges or at the intersections of the cuts, indicating stronger adhesion was attained without decreasing the electrical conductivity.

From the standpoint of chemical structures of the alkanol-amine ligands (AB and AmIP) in the Cu NPs examined in our study, it was possible that the primary or secondary alcohol of the alkanol-amine ligands had a close relationship with the residual oxidation products inside the sintering Cu films. The increased adhesiveness of the nanoink

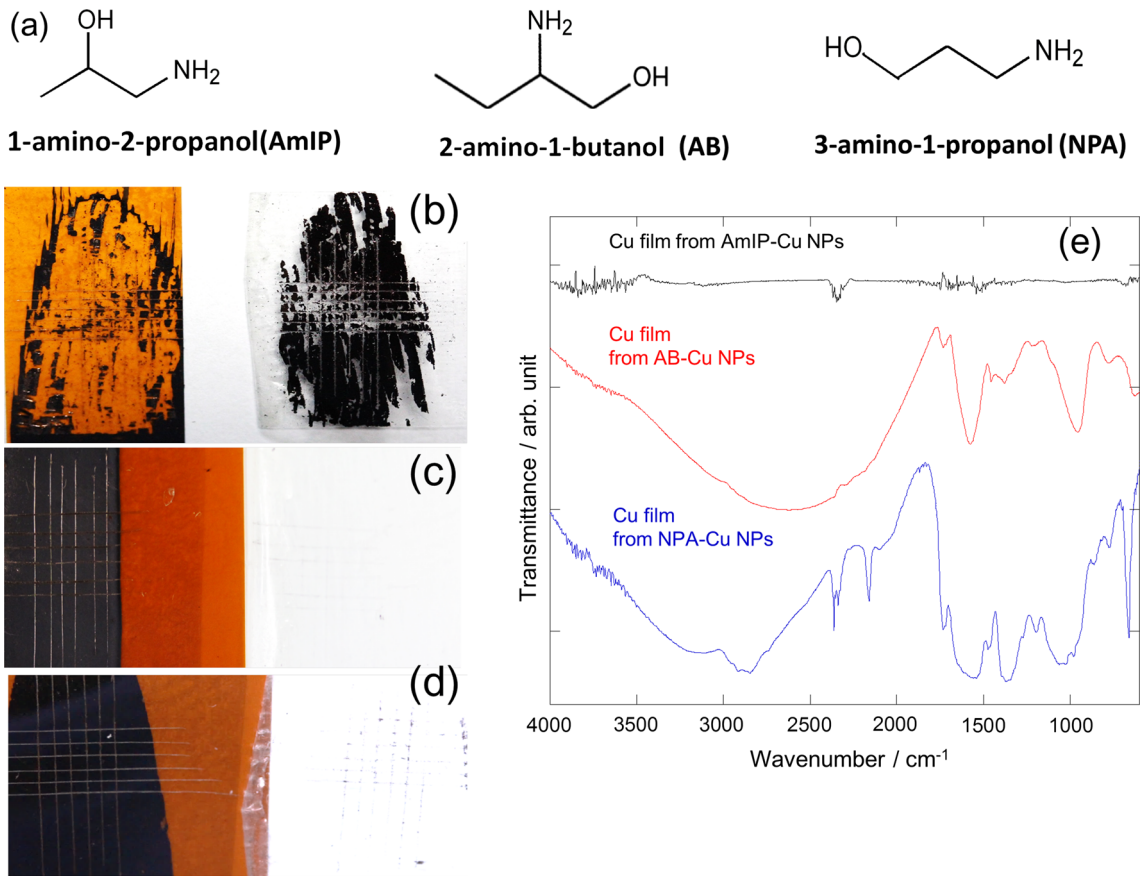

Fig. 6 **a** Chemical structures of AmIP, AB, and NPA. **b–d** Adhesion strength test of the Cu film on a polyimide film. Different Cu films were prepared by the thermal sintering of **b** AmIP-Cu NP nanoink, **c** AB-Cu NP nanoink, and **d** NPA-Cu NP nanoink (~35 wt% Cu, propylene glycol/glycerol solvent = 1:1 v/v) for 30 min at a temperature of 150 °C. The triple cross-cut test was conducted on the Cu films. **e** IR spectra of Cu films prepared from the AmIP-Cu NP nanoink, AB-Cu NP nanoink, and NPA-Cu NP nanoink

based on AB-Cu NPs (compared to that of the nanoink based on Am IP-Cu NPs) was probably due to the presence of residual oxidation products after the thermal sintering of the Cu nanoink (as shown in the TG analysis), which strengthened the adhesion of the Cu film to the substrate. We analysed the oxidation products inside the sintering Cu films prepared from the AB-Cu NP nanoink by IR spectroscopy (Fig. 6e). The results revealed distinct IR peaks from residual organic molecules in the sintering Cu film from the AB-Cu NP nanoink, which are in sharp contrast to the spectrum of the Cu film prepared from the AmIP-Cu NP nanoink. Unlike the O–H stretching band observed in alcohols, the O–H stretching of carboxylic acid appears as a very broad band in the range of 3300–2300 cm^{-1}, and the C=O carbonyl stretching of the carboxylic acid appears as intense bands in the range of 1700–1625 cm^{-1}. The IR spectrum indicates the presence of compounds associated with the carboxylic acid inside the sintering Cu film prepared from the AB-Cu NP nanoink; these compounds could have been produced by the oxidation of the primary alcohol in AB ligands during the thermal sintering process. It is likely that the carboxylic-acid-based compounds from the AB-Cu NPs improved the adhesion of the Cu film to the PI film.

Since the NPA ligands also have a primary alcohol, resulting in oxidation products in the form of carboxylic acids, it is reasonable that the sintering Cu film prepared from the NPA-Cu NP nanoink also showed improved adhesion, which is similar to the case of the Cu film prepared from the AB-Cu NP nanoink. In fact, the presence of carboxylic compounds in the sintering Cu films prepared from NPA-Cu NP-based nanoink was also confirmed by IR spectroscopy (Fig. 6e); the adhesion strength dramatically improved in the Cu film prepared from the NPA-Cu NP nanoink (Fig. 6d). However, high electrical resistivity was obtained for the Cu film prepared from the NPA-Cu NP nanoink: a non-conductive Cu film with high electrical resistivity ($\sim 10^1$ Ω cm) was obtained for the film prepared from the NPA-Cu NP nanoink even after sintering at the high temperature of 200 °C, whereas the conductive Cu film with the low electrical resistivity (~ 20 μΩ cm) was derived from the AB-Cu NP nanoink. The reason for the conflicting nature of the Cu films prepared from the NPA-Cu NP nanoink and the AB-Cu NP nanoink remains unclear because the chemical structures of the carboxylic compounds from AB-Cu NPs and NPA-Cu NPs could not be identified in the present study.

Our study demonstrated that the Cu film prepared from the AmIP-Cu NP nanoink showed vanishingly small amount of residual organic products after the heat treatment at 150 °C (Fig. 6e), which is in contrast to the films prepared from nanoinks of AB-Cu NPs and NPA-Cu NPs. The secondary alcohol of AmIP might have been oxidized to ketones during the heating process, and the ketone products would have been easily removed by heating because of their low boiling points, resulting in very weak adhesion of the Cu film prepared from the AmIP-Cu NP nanoink to the substrate. Several mechanisms have been proposed for the oxidative degradation of alkanol-amine molecules [40]. One of the proposed reaction pathways is based on the formation of cyclic ring structures containing O···H or N···H bonds, resulting in cyclic compounds [40]. In fact, pyrolysis-gas chromatography–mass spectrometry (pyrolysis-GC–MS) analysis of the Cu film prepared from the AmIP-Cu NP nanoink suggested the presence of cyclic compounds (e.g. pyrazine compounds) inside the film (ESI Fig. S4). Details of the oxidation or degradation pathway of the alkanol-amine molecules during thermal sintering of Cu NPs should be recognized as an important subject that is open for consideration in the fabrication of Cu nanoinks.

4 Conclusions

High-concentration (0.3 M copper salt) synthesis of AB-Cu NPs with an average size of 4.4 ± 1.0 nm was carried out in ethylene glycol at the room temperature under ambient air conditions, using the metallacyclic coordination stability of a five-membered ring type between Cu and the AB ligand. The sintering-temperature of 60 °C for the AB-Cu NPs is the lowest value ever reported for Cu NPs. The nanoink based on these AB-Cu NPs (~35 wt% Cu) produced a conductive Cu film with resistivity of 52 μΩ cm after low-temperature heating at 150 °C under a nitrogen flow. This Cu film established strong adhesion to the substrate without decreasing the electrical conductivity, but the films prepared from the other Cu nanoinks consisting of AmIP-Cu NPs displayed weak adhesion to the substrate. The adhesiveness of the AB-based Cu nanoink is attributed to the carboxylic compounds produced after the thermal sintering of the Cu nanoinks, which depended on the primary or secondary alcohol of the alkanol-amine stabilizers used to synthesize the Cu NPs.

Acknowledgments We thank Mr. Daisuke Murahashi and Ms. Kazuko Yamashita at Kansai University for the GC–MS measurements. This work was supported by JSPS KAKENHI (Grant Nos. 15H03520, 15H03526, 26505011 and 26107719) and Hitachi Metals Materials Science Foundation.

References

1. S. Magdassi, M. Grouchko, A. Kamyshny, Materials **3**, 4626 (2010)
2. K. Tanabe, Mater. Lett. **61**, 4573 (2007)

3. Y. Isomura, T. Narushima, H. Kawasaki, T. Yonezawa, Y. Obora, Chem. Commun. **48**, 3784 (2012)
4. J. Ramyadevi, K. Jeyasubramanian, A. Marikani, G. Rajakumar, A. Rahuman, Mater. Lett. **71**, 114 (2012)
5. V. Abhinav, V.K.R. Rama, K.P. Selvam, S.P. Singh, RSC Adv. **5**, 63985 (2015)
6. C.Y. Lai, C.F. Cheong, J.S. Mandeep, H.B. Abdullah, N. Amin, K.W. Lai, J. Mater. Eng. Perform. **23**, 3541 (2014)
7. Y. Jo, S.J. Oh, S.S. Lee, Y.H. Seo, B.H. Ryu, J. Moon, Y. Choi, S. Jeong, J. Mater. Chem. C **2**, 9746 (2014)
8. M. Hauder, J. Gstöttner, W. Hansch, D. Schmitt-Landsiedel, Appl. Phys. Lett. **78**, 838 (2001)
9. B.K. Park, D. Kim, S. Jeong, J. Moon, J.S. Kim, Thin Solid Films **19**, 7706 (2007)
10. Y. Lee, J.R. Choi, K.J. Lee, N.E. Stott, D. Kim, Nanotechnology **19**, 415604 (2008)
11. N.A. Luechinger, E.K. Athanassiou, W.J. Stark, Nanotechnology **19**, 445201 (2008)
12. H.S. Kim, S.R. Dhage, D.E. Shim, H.T. Hahn, Appl. Phys. A **97**, 791 (2009)
13. J.S. Kang, H.S. Kim, J. Ryu, H.T. Hahn, S. Jang, J.W. Joung, J. Mater. Sci.: Mater. Electron. **21**, 1213 (2010)
14. S. Jang, Y. Seo, J. Choi, T. Kim, J. Cho, S. Kim, D. Kim, Scr. Mater. **62**, 258 (2010)
15. Y. Jianfeng, Z. Guisheng, H. Anming, Y.N. Zhou, J. Mater. Chem. **21**, 15981 (2011)
16. K. Woo, Y. Kim, B. Lee, J. Kim, J. Moon ACS Appl. Mater. Interfaces **3**, 2377 (2011)
17. C.S. Choi, Y.H. Jo, M.G. Kim, H.M. Lee, Nanotechnology **23**, 065601 (2012)
18. C.-J. Wu, S.-M. Chen, Y.-J. Sheng, H.-K. Tsao, J. Taiwan Inst. Chem. Eng. **45**, 2719 (2014)
19. W. Li, M. Chen, Appl. Surf. Sci. **290**, 240 (2014)
20. C.-J. Wu, S.-L. Cheng, Y.-J. Sheng, H.-K. Tsao, RSC Adv. **5**, 53275 (2015)
21. Y. Yong, T. Yonezawa, M. Matsubara, H. Tsukamoto, J. Mater. Chem. C **3**, 5890 (2015)
22. T. Yonezawa, H. Tsukamoto, Y. Yong, M. Thanh Nguyen, M. Matsubara, RSC Adv. **6**, 12048 (2016)
23. D.M. Kalyon, E. Birinci, R. Yazici, B. Karuv, S. Walsh, Polym. Eng. Sci. **42**, 1609 (2002)
24. Y. Hokita, M. Kanzaki, T. Sugiyama, R. Arakawa, H. Kawasaki, A.C.S. Appl, Mater. Interfaces **7**, 19382 (2015)
25. P.A. Buffat, J.P. Borel, Phys. Rev. A **13**, 2287 (1976)
26. S.H. Wu, D.H. Chen, J. Colloid Interface Sci. **273**, 165 (2004)
27. P. Kanninen, C. Johans, J. Merta, K. Kontturi, J. Colloid Interface Sci. **318**, 88 (2008)
28. J.L.C. Huaman, K. Sato, S. Kurita, T. Matsumoto, B. Jeyadevan, J. Mater. Chem. **21**, 7062 (2011)
29. D. Deng, Y. Cheng, Y. Jin, T. Qi, F. Xiao, J. Mater. Chem. **22**, 23989 (2012)
30. J. Mittal, K.-L. Lin, Mater. Charact. **109**, 19 (2015)
31. J.W.M. Frenken, J.F. Vanderveen, Phys. Rev. Lett. **54**, 134 (1985)
32. F.W. Young, J.V. Cathcart, A.T. Gwathmey, Acta Metall. **4**, 145 (1956)
33. K.K. Jee, W.Y. Lee, J. Korean Phys. Soc. **52**, 1673 (2008)
34. I. Kim, Y.A. Song, H.C. Jung, J.W. Joung, S.-S. Ryu, J. Kim, J. Electron. Mater. **37**, 1863 (2008)
35. J.-K. Jung, S.H. Choi, I. Kim, H.C. Jung, J. Joung, Y.-C. Joo, Philos. Mag. **88**, 339 (2008)
36. I. Kim, J. Kim, J. Appl. Phys. **108**, 102807 (2010)
37. I. Jung, Y.H. Jo, I. Kim, H.M. Lee, J. Electron. Mater. **41**, 115 (2012)
38. I. Kim, T.-M. Lee, J. Kim, J. Alloys Compd. **596**, 158 (2014)
39. Y. Kim, B. Lee, S. Yang, I. Byun, I. Jeong, S.M. Cho, Curr. Appl. Phys. **12**, 473 (2012)
40. S.B. Fredriksen, K.-J. Jens, Energy Procedia **37**, 1770 (2013)